Asymmetric transmission of terahertz waves through a graphene-loaded metal grating

Yu Zhou, Ye-Qing Dong, Ren-Hao Fan, Qing Hu, Ru-Wen Peng, and Mu Wang

Citation: Applied Physics Letters **105**, 041114 (2014); doi: 10.1063/1.4891818
View online: http://dx.doi.org/10.1063/1.4891818
View Table of Contents: http://scitation.aip.org/content/aip/journal/apl/105/4?ver=pdfcov
Published by the AIP Publishing

Asymmetric transmission of terahertz waves through a graphene-loaded metal grating

Yu Zhou,[1] Ye-Qing Dong,[1] Ren-Hao Fan,[1] Qing Hu,[1,2] Ru-Wen Peng,[1,a)] and Mu Wang[1]
[1]*National Laboratory of Solid State Microstructures and Department of Physics, National Center of Microstructures and Quantum Manipulation, Nanjing University, Nanjing 210093, China*
[2]*Department of Mechanical Engineering, Massachusetts Institute of Technology, Cambridge, Massachusetts 02139, USA*

(Received 10 May 2014; accepted 20 July 2014; published online 30 July 2014)

In this work, we theoretically investigate the propagation of terahertz (THz) waves through a graphene-loaded metal grating under external magnetic field. It is found that resonant modes in the system can be converted between transverse-electric and transverse-magnetic polarizations due to Hall conductivity of graphene. As a consequence, asymmetric transmission of THz waves through this graphene-loaded metal grating is achieved. Furthermore, by adjusting either the external magnetic field or the Fermi level of graphene, such asymmetric wave propagation can be significantly tuned. The investigations may provide a unique way to achieve the graphene-loaded optodevices for THz waves. © *2014 AIP Publishing LLC*. [http://dx.doi.org/10.1063/1.4891818]

In recent years, there has been considerable interest in asymmetric wave propagation.[1–20] Several approaches have been proposed. One typical way is to break time-reversal symmetry in the system,[1–8] as is achieved in Faraday isolators.[21] It is known that time-reversal operation on the electromagnetic fields can be carried out by conjugation of complex amplitudes and the inversion of wave vectors. Thus, in a gyrotropic medium,[22] the Jones matrix of electromagnetic waves in one direction is not transposed to that of the reverse direction, which directly leads to asymmetric transmission, or more specifically, to non-reciprocity in the wave propagation. Another approach for achieving asymmetric wave propagation is to break the inversion symmetry in the system.[9–13] For example, if a system has different periods of slits on two sides, the diffracted beams will emanate from one surface only, thus one-way resonant diffraction grating is produced.[9,10] In addition, nonlinearity has also been introduced into the system in order to generate asymmetry in the wave propagation.[14–18]

Asymmetric wave propagation has many potential applications in developing photonic materials and opto-devices, such as optical isolators and optical diodes, particularly for optical integrated circuits. Most works in this area are explored at visible, infrared, and microwave regimes. However, little attention has been paid to asymmetric transmission of terahertz (THz) waves. The THz waves, which cover the frequencies from 10^{11} to 10^{13} Hz, can bridge the gap between the infrared and the microwaves in the electromagnetic spectrum. The THz technology[23–25] has been applied in information and communications, imaging and sensing, biology and medical sciences, homeland security, and so on. In order to contribute to these applications, one of the key points is to manipulate the transmission of THz waves efficiently and actively, yet many challenges still need to be overcome. For example, few THz devices could realize one-way transmission up to now, which is particularly desired for THz wave isolators. In this work, we propose an approach to achieve asymmetric transmission of THz waves based on a graphene-loaded structure. It is known that graphene is becoming a promising platform for photonics and plasmonics.[26–28] By applying an external magnetic field, graphene has presented Hall conductivity and Faraday rotation.[29–33] Here, we try to realize one-way transmission for polarized THz waves by relying on Faraday effect in graphene. We will demonstrate that in a graphene-loaded metal grating, the transverse-electric (TE) modes are converted to the transverse-magnetic (TM) modes in the forward transmission; but fail in the backward propagation. Thus, asymmetric transmission of THz waves through this graphene-loaded metal grating is achieved. Furthermore, by adjusting either the external magnetic field or the Fermi level of the graphene, asymmetric wave propagation can be significantly tuned in the system. The theoretical investigations may provide a unique approach to actively control the propagation of THz waves and have potential applications on the graphene-loaded optodevices at THz regime.

As schematically illustrated in Fig. 1, we intentionally arrange a single-layer graphene on one side of a perfect electric conductor (PEC) grating, and apply an external magnetic field perpendicular to the graphene. In Fig. 1, the grey area indicates the PEC grating with the stripes along the x axis, and a graphene sheet is located on the left side of the PEC grating (parallel to xy plane). A magnetic field B (indicated by a grey arrow) is applied along the z axis. For simplicity, we assume that all the dielectrics in the system are vacuum. The period, thickness, and width of the grating slits are denoted as p, h, and d, respectively. The spacing between graphene and grating is denoted as D. For simplicity, we define the wave propagation toward the $+z$ axis as the forward transmission; while the wave propagation toward the $-z$ axis is defined as the backward transmission.

TE-polarized and TM-polarized waves will propagate asymmetrically through the system we have designed. Physically, if TE-polarized THz waves are incident from region I (the left side) of the system (as shown in Fig. 1(a)),

a)Author to whom correspondence should be addressed. Electronic mail: rwpeng@nju.edu.cn

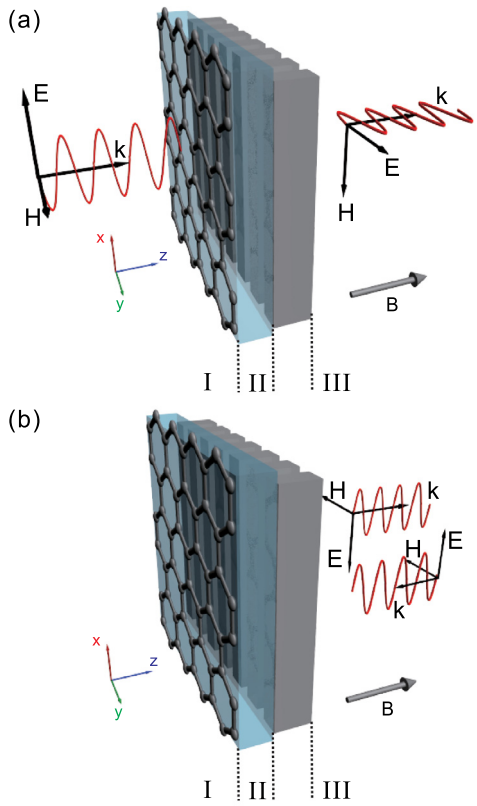

FIG. 1. Schematics of asymmetric propagation of the TE-polarized waves through the system with graphene loaded on a PEC grating if the external magnetic field (B) is applied. (a) Forward propagation of the wave at normal incidence from region I; (b) Backward propagation of the wave at normal incidence from region III. For simplicity, all the dielectrics in the system (including region II) are assumed to be vacuum.

due to the Faraday rotation of graphene, the TE modes will be partially converted into TM modes, thereafter, the TM modes will go through the PEC grating and finally contribute to the forward transmission. However, if TE-polarized THz waves are incident from region III (the right side) of the system, the PEC grating will stop their propagation and then reflect them back, thus no backward transmission will be observed (as shown in Fig. 1(b)). In this way, asymmetric transmission for the TE-polarized waves can be realized. As for TM-polarized THz waves, the physical process is as follows. When TM-polarized waves are incident from region I, graphene will convert some of the TM modes into TE modes, but those TE modes cannot go through the PEC grating. As a result, along the forward direction (i.e., $+z$ axis), TM modes can be detected but no TE modes will be observed. On the other hand, if TM-polarized waves are incident from region III, the TM modes will go through the PEC grating, and then some of the TM modes will be converted into TE modes. Thereafter, along the backward direction (i.e., $-z$ axis), both TM modes and TE modes will be observed. Therefore, asymmetric transmission for the TM-polarized waves can also be realized.

The above wave propagation can be analyzed based on the S-matrix method.[1,2] The S matrix of the whole system can be derived by using iteration process based on the wave propagation through both graphene and grating. First, we consider the THz waves going through graphene. In the THz region, graphene can be treated as an infinitesimally thin conductive layer that has a two-dimensional conductivity tensor[29–33]

$$\vec{\sigma} = \begin{pmatrix} \sigma_{xx} & \sigma_{xy} \\ \sigma_{yx} & \sigma_{yy} \end{pmatrix} = \begin{pmatrix} \sigma_l & \sigma_h \\ -\sigma_h & \sigma_l \end{pmatrix}, \tag{1}$$

if a static magnetic field is applied perpendicularly to the graphene plane. Here, σ_l and σ_h are the longitudinal conductivity and the Hall conductivity of the graphene, respectively. Due to the symmetry, the two diagonal terms are identical while the two off-diagonal terms have opposite signs. In the presence of Hall conductivity, the Faraday effect may arise, which will mix the x and y polarizations and cause polarization conversion. In order to calculate the transmission of THz waves through graphene, the traditional S matrix must be extended into a vector form. We derive the S matrix of graphene by imposing two boundary conditions: one, that the tangential components of the electric field are continuous across the graphene; and two, that the discontinuity of the magnetic field at two sides of the graphene equals the surface current. Thus, we have

$$\begin{cases} \vec{E}_F^{(I)} + \vec{E}_B^{(I)} = \vec{E}_F^{(II)} + \vec{E}_B^{(II)}, \\ \vec{H}_F^{(I)} + \vec{H}_B^{(I)} - \vec{H}_F^{(II)} - \vec{H}_B^{(II)} = \frac{1}{2}\mathbf{T}\vec{\boldsymbol{\sigma}}(\vec{E}_B^{(I)} + \vec{E}_F^{(I)} + \vec{E}_B^{(II)} + \vec{E}_F^{(II)}), \end{cases} \tag{2}$$

where $\vec{E}_F^{(i)}/\vec{H}_F^{(i)}$ and $\vec{E}_B^{(i)}/\vec{H}_B^{(i)}$ are the electric/magnetic fields propagating forward and backward in the region i (i = I or II), respectively. Here, the subscripts "F" and "B" are for forward and backward propagating waves, respectively. The matrix $\mathbf{T}$ is defined as

$$\mathbf{T} = \begin{bmatrix} 0 & -1 \\ 1 & 0 \end{bmatrix}. \tag{3}$$

The magnetic fields in forward and backward directions in region i (i = I or II) can be derived by

$$\begin{pmatrix} H_{x,F}^{(i)} \\ H_{y,F}^{(i)} \end{pmatrix} = \mathbf{T}_{he,F}^{(i)} \begin{pmatrix} E_{x,F}^{(i)} \\ E_{y,F}^{(i)} \end{pmatrix}, \quad \begin{pmatrix} H_{x,B}^{(i)} \\ H_{y,B}^{(i)} \end{pmatrix} = \mathbf{T}_{he,B}^{(i)} \begin{pmatrix} E_{x,B}^{(i)} \\ E_{y,B}^{(i)} \end{pmatrix}, \tag{4}$$

respectively. Here, $\mathbf{T}_{he,F}^{(i)}$ and $\mathbf{T}_{he,B}^{(i)}$ are the matrices that transform the forward and backward propagating electric fields into the corresponding magnetic fields, respectively. By solving Eqs. (2) and (4), the S matrix of graphene can be derived as

$$\begin{pmatrix} \vec{E}_B^{(I)} \\ \vec{E}_F^{(II)} \end{pmatrix} = \begin{pmatrix} \mathbf{S}_{11} & \mathbf{S}_{12} \\ \mathbf{S}_{21} & \mathbf{S}_{22} \end{pmatrix} \begin{pmatrix} \vec{E}_F^{(I)} \\ \vec{E}_B^{(II)} \end{pmatrix}, \tag{5}$$

where the four elements of the S matrix are $\mathbf{S}_{11} = (\mathbf{T}_{he,B}^{(I)} - \mathbf{T}_{he,F}^{(II)} - \mathbf{T}\vec{\boldsymbol{\sigma}})^{-1}(\mathbf{T}_{he,F}^{(II)} - \mathbf{T}_{he,F}^{(I)} + \mathbf{T}\vec{\boldsymbol{\sigma}})$, $\mathbf{S}_{12} = (\mathbf{T}_{he,B}^{(I)} - \mathbf{T}_{he,F}^{(II)} - \mathbf{T}\vec{\boldsymbol{\sigma}})^{-1}(\mathbf{T}_{he,B}^{(II)} - \mathbf{T}_{he,F}^{(II)})$, $\mathbf{S}_{21} = (\mathbf{T}_{he,B}^{(I)} - \mathbf{T}_{he,F}^{(II)} - \mathbf{T}\vec{\boldsymbol{\sigma}})^{-1}(\mathbf{T}_{he,B}^{(I)} - \mathbf{T}_{he,F}^{(I)})$, and $\mathbf{S}_{22} = (\mathbf{T}_{he,B}^{(I)} - \mathbf{T}_{he,F}^{(II)} - \mathbf{T}\vec{\boldsymbol{\sigma}})^{-1}(\mathbf{T}_{he,B}^{(II)} - \mathbf{T}_{he,B}^{(I)} + \mathbf{T}\vec{\boldsymbol{\sigma}})$, respectively.

Now we consider a PEC grating and derive the S matrix for the grating. In the case where both the grating period and the slit width are much smaller than the wavelength, only the TM-polarized waves can be partially transmitted through the

grating while the TE-polarized waves are completely reflected. For simplicity, we only consider the zero-order diffraction. In the graphene-loaded grating system (shown in Fig. 1), mainly due to the fact that under normal incidence these two types of polarizations are not coupled in the grating, we can calculate the S matrices for x components and y components of the electric fields independently and then we recombine them into a vector form. In the grating, the x components of electric fields follow:

$$\begin{cases} E_{x0,F}^{(II)} + E_{x0,B}^{(II)} = 0, \\ E_{x0,F}^{(III)} e^{ik_{zn}^{(III)}h} + E_{x0,B}^{(III)} e^{-ik_{zn}^{(III)}h} = 0, \end{cases} \tag{6}$$

where $E_{x0,F}^{(i)}$ and $E_{x0,B}^{(i)}$ denote the x components of the electric fields during forward and backward propagation of the zero-order diffracted waves in the i ($i = $ II or III) region at the two sides of the grating, respectively. By solving for $E_{x0,F}^{(II)}$ and $E_{x0,B}^{(III)}$ in Eq. (6), one can determine the S matrix for the x components of the electric field. As for the y components, we must consider the TM modes in the grating slits.[34–38] By solving these equations, one can derive the S matrix for the grating as

$$\begin{pmatrix} E_{x0,B}^{(II)} \\ E_{y0,B}^{(II)} \\ E_{x0,F}^{(III)} \\ E_{y0,F}^{(III)} \end{pmatrix} = \begin{pmatrix} S_{11}^{TE} & 0 & S_{12}^{TE} & 0 \\ 0 & S_{11}^{TM} & 0 & S_{12}^{TM} \\ S_{21}^{TE} & 0 & S_{22}^{TE} & 0 \\ 0 & S_{21}^{TM} & 0 & S_{22}^{TM} \end{pmatrix} \begin{pmatrix} E_{x0,F}^{(II)} \\ E_{y0,F}^{(II)} \\ E_{x0,B}^{(III)} \\ E_{y0,B}^{(III)} \end{pmatrix}. \tag{7}$$

More explicitly, we have

$$\mathbf{S}^{TE} = \begin{pmatrix} S_{11}^{TE} & S_{12}^{TE} \\ S_{21}^{TE} & S_{22}^{TE} \end{pmatrix} = \begin{pmatrix} -1 & 0 \\ 0 & -1 \end{pmatrix} \tag{8}$$

and

$$\mathbf{S}^{TM} = \begin{pmatrix} S_{11}^{TM} & S_{12}^{TM} \\ S_{21}^{TM} & S_{22}^{TM} \end{pmatrix} = \begin{pmatrix} r_0 & t_0 \\ t_0 & r_0 \end{pmatrix}, \tag{9}$$

where r_0 and t_0 are the reflection and transmission coefficients for the zero-order diffracted TM-polarized waves, respectively.

Based on the S-matrix approach described above, we carry out the numerical calculations for THz transmission in the graphene-loaded grating system. In the following calculations, all of the values for the conductivity tensors in graphene are obtained by using the formulas in Ref. 29. The temperature is set at $T_{temp} = 300\,\mathrm{K}$ and the damping constant is set at $\Gamma = 6.8\,\mathrm{meV}$. Spatial dispersion is neglected because we focus on the low THz region.[32] In order to thoroughly explore the asymmetric features of the transmission, we have defined four transmission components: T_{xx}, T_{xy}, T_{yx}, and T_{yy}. Here, T_{ij} ($i = x,y$ and $j = x,y$) indicates the ratio of the transmitted intensity of the j-polarized wave to the incident intensity of the i-polarized wave, i.e., $T_{ij} = |E_j|^2/|E_i|^2$.

As shown in Figs. 2(a) and 2(b), if the TE-polarized (i.e., x-polarized) THz waves are incident on region I, graphene converts some of these TE modes into TM (i.e., y-polarized) modes. Thereafter, the remaining TE modes are stopped by the PEC grating, which leads to all T_{xx} being zero (see Fig. 2(a)); but the TM modes can go through the PEC grating, which contributes to nonzero forward transmission, e.g., $T_{xy} \sim 0.08$ at 1.5 THz (see Fig. 2(b)). However, if the TE-polarized THz waves are incident on region III, the PEC grating stops their propagation and reflects them back, thus no backward transmission can be observed (as shown in Figs. 2(a) and 2(b)). Therefore, as demonstrated by T_{xy} in Fig. 2(b), asymmetric transmission for the TE-polarized THz waves is achieved in the graphene-loaded grating system. On the other hand, if the TM-polarized (i.e., y-polarized) waves are incident on region I, some of them are converted into the TE modes by the graphene, but those TE modes fail to go through the PEC grating. As a result, along the forward direction, no TE modes are observed, which leads to all T_{yx} being zero (see Fig. 2(c)), but the remaining TM modes are detected (see Fig. 2(d)). While if TM-polarized waves are incident from the region III, the TM modes go through the PEC grating, and then some of the TM modes are converted into TE modes. Thereafter, along the backward direction, both TM and TE modes are observed. Thus, as demonstrated by T_{yx} in Fig. 2(c), asymmetric transmission for the TM-polarized THz waves is also achieved in this system.

In order to provide more evidence of asymmetric propagation in the system, we have calculated the THz transmission and reflection spectra for x/y-polarized incident waves (as shown in Fig. 3). It is shown that asymmetric transmission indeed happens for the x-polarized THz waves (see Fig. 3(a)), but such asymmetric effect becomes extremely weak for the y-polarized waves (see Fig. 3(b)). However, asymmetric reflection occurs for both x-polarized and y-polarized THz waves (see Figs. 3(c) and 3(d)). If we denote that T_f and T_b are the transmission intensities for forward and backward propagation, respectively, the contrast between the forward and backward transmissions can be defined as $C = (T_f - T_b)/(T_f + T_b) \times 100\%$. Obviously, for the x-polarized incident waves, only forward propagation is permitted, therefore the contrast between forward and backward transmission can reach 100%. But for the y-polarized incident waves, the contrast is much lower, about 6.7% at 1.53 THz, mainly because high transmission is achieved for both the forward and backward directions. It should be noted that the forward transmission shown in Figs. 2(b) and 3(a) is very limited due to monolayer graphene. Although Graphene has giant Hall conductivity, Faraday rotation is limited in monolayer graphene because the rotation angle is proportional to the distance travelled by the light. For example, for a graphene sheet on *SiC*, the rotation angle is about 0.1 rad under an applied magnetic field $B = 7\,\mathrm{T}$ and a temperature $T = 5\,\mathrm{K}$.[30,31] To enlarge the Faraday rotation, one may use N-layer graphene sheets instead of monolayer graphene, which can enhance the conductivity to be N multiples. In this way, the polarization conversion can be significantly improved. There are other ways to enhance the Faraday rotation such as increasing the Fermi level and fabricating graphene metasurfaces with different shapes.[32] Further studies are still carried on to obtain stronger forward transmission by increasing the Faraday rotation in the system.

One advantage of graphene over other materials is that it can be easily tuned either by the external magnetic field or

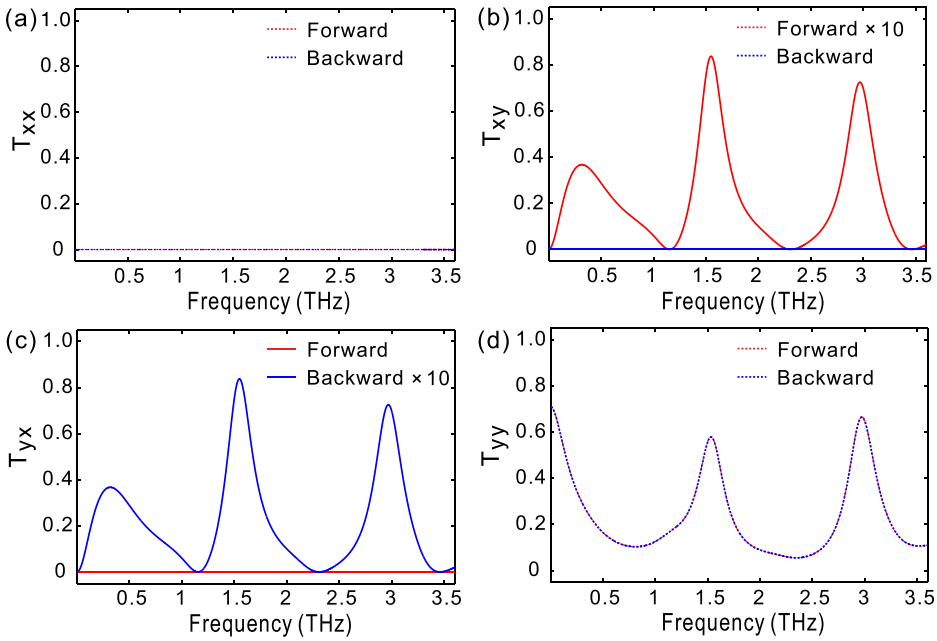

FIG. 2. The transmission components as a function of frequencies in the graphene-loaded PEC grating system: (a) T_{xx}, (b) T_{xy}, (c) T_{yx}, and (d) T_{yy}. Red curves show the forward propagation (along the $+z$ direction) and blue curves show the backward propagation (along the $-z$ direction). Here, the grating in the system has the period $p = 50\ \mu$m, the thickness $h = 100\ \mu$m, and the slit width $d = 10\ \mu$m. The spacing between graphene and grating is $D = 80\ \mu$m. The applied magnetic field is $B = 5$ T and the Fermi level of the graphene is $\mu = 0.3$ eV.

by the Fermi level, thus remarkably changes its response to the electromagnetic waves. This feature enables us to design tunable graphene-loaded THz devices. As we know, graphene possesses both longitudinal conductivity and Hall conductivity under magnetic field. By tuning the conductivity tensor of graphene, the polarization conversion of the THz wave can be changed, thus asymmetric transmission can be actively tuned in our system. Figure 4 shows the transmission component T_{xy} at the first three peaks in the forward propagation for different magnetic fields and Fermi levels. Under specific magnetic field, increasing the Fermi level will enhance the asymmetric transmission of the THz waves (as shown in Fig. 4(a)). This enhancement can be attributed to the increasing of electron density and the conductivity of graphene which leads to stronger electromagnetic responses. Actually such external tuning effect can be performed over GHz frequencies. On the other hand, varying the magnetic field will also tune the resonant transmissions, see Fig. 4(b). The peaks and nodes in the T_{xy} spectra actually originate from the Fabry-Perot (FP) resonances in the structure. There mainly exist two FP resonances: one is within the grating and the other is between the graphene and the grating. Thus, the resonant peaks and nodes can be easily tuned by adjusting the geometry parameters. Here, we change the spacing between graphene and grating, denoted as D, and the thickness of grating, denoted as h. As shown in Fig. 5, the resonant peaks and nodes are significantly modified in the transmission spectra by increasing the grating thickness h and the spacing D. These FP resonances can be employed to maximize the asymmetric transmission at specific frequencies. Particularly, the position of the asymmetric transmission peaks can be tuned by the grating thickness h, and the intensity of the asymmetric transmission peaks can be maximized by tuning the spacing D. In this way, asymmetric propagation of THz wave can be significantly tuned in our graphene-loaded PEC grating.

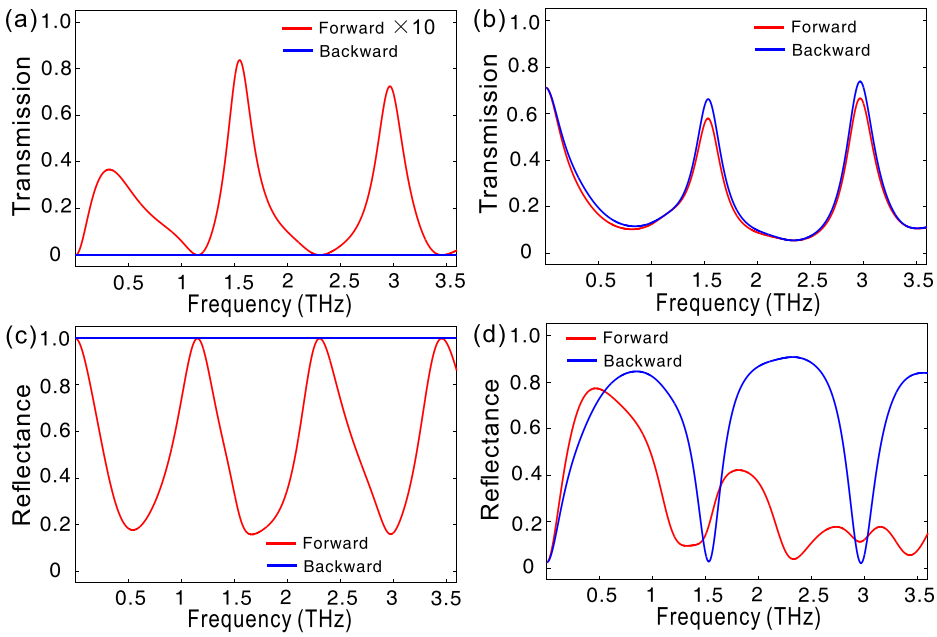

FIG. 3. Transmission spectra for different polarizations in the graphene-loaded PEC grating system: (a) x-polarized (i.e., TE waves); and (b) y-polarized (i.e., TM waves). And reflection spectra for different polarizations in the same system: (c) x-polarized; and (d) y-polarized. Red curves show the forward propagation and blue curves show the backward propagation. The geometric parameters in the system are the same as those in Fig. 2.

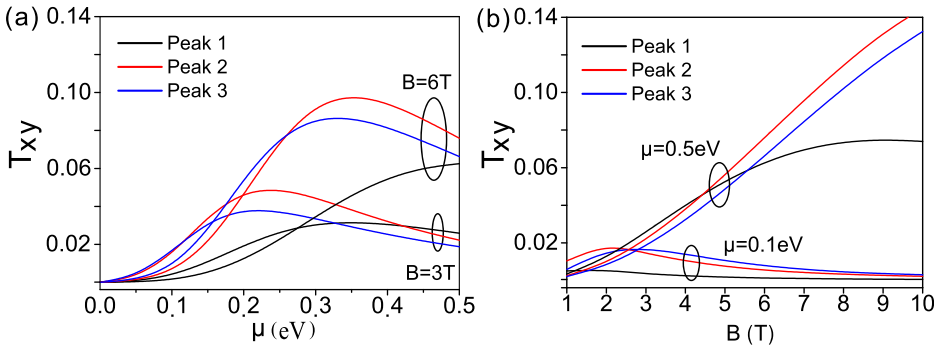

FIG. 4. (a)The transmission component T_{xy} at the lowest three resonant peaks as a function of the Fermi levels of graphene (μ) under different magnetic fields (B). (b) The transmission component T_{xy} at the lowest three resonance peaks as a function of the magnetic fields (B) under different Fermi levels of graphene (μ). The geometric parameters in the system are the same as those in Fig. 2. Please note that all cases are in forward propagation.

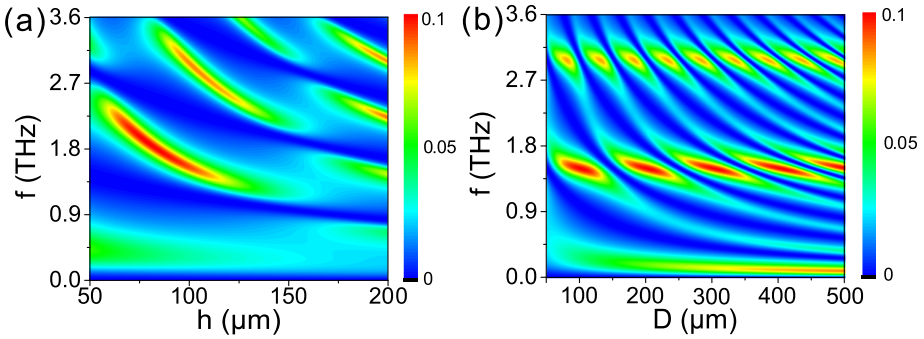

FIG. 5. (a) Transmission component T_{xy} as a function of frequencies in the graphene-loaded PEC grating systems with different grating thicknesses (h). Here, $p = 50$ μm, $d = 10$ μm, and $D = 80$ μm. (b) Transmission component T_{xy} as a function of frequencies in the systems with different spacing (D) between graphene and grating in the systems. Here, $p = 50$ μm, $h = 100$ μm, and $d = 10$ μm. Please note that all cases are in forward propagation under the magnetic field $B = 6$ T and the Fermi level of the graphene $\mu = 0.3$ eV.

In summary, we have theoretically demonstrated asymmetric propagation of THz waves through a graphene-loaded metal grating under external magnetic fields. By relying on the Faraday effect of graphene, the resonant modes in the system can be converted between TE and TM polarizations; as a result, asymmetric transmission and reflection of THz waves are achieved. Furthermore, by adjusting either the external magnetic field or the Fermi level of graphene, asymmetric wave propagation can be significantly tuned. These investigations offer a unique approach to manipulate the propagation of THz waves, which has potentially applications in the design of the graphene-loaded tunable devices such as THz isolators and diodes.

This work was supported by the Ministry of Science and Technology of China (Grant Nos. 2012CB921502 and 2010CB630705), and the National Natural Science Foundation of China (Grant Nos. 11034005, 11321063, and 91321312).

[1]A. Figotin and I. Vitebsky, Phys. Rev. E **63**, 066609 (2001).
[2]A. Figotin and I. Vitebskiy, Phys. Rev. B **67**, 165210 (2003).
[3]Z. F. Yu, Z. Wang, and S. H. Fan, Appl. Phys. Lett. **90**, 121133 (2007).
[4]H. Takeda and S. John, Phys. Rev. A **78**, 023804 (2008).
[5]Z. F. Yu, G. Veronis, Z. Wang, and S. H. Fan, Phys. Rev. Lett. **100**, 023902 (2008).
[6]A. Christofi and N. Stefanou, Phys. Rev. B **87**, 115125 (2013).
[7]D. W. Wang, H. T. Zhou, M. J. Guo, J. X. Zhang, J. Evers, and S. Y. Zhu, Phys. Rev. Lett. **110**, 093901 (2013).
[8]H. Y. Dong, J. Wang, and T. J. Cui, Phys. Rev. B **87**, 045406 (2013).
[9]M. J. Lockyear, A. P. Hibbins, K. R. White, and J. R. Sambles, Phys. Rev. E **74**, 056611 (2006).
[10]Z. J. He, S. S. Peng, Y. T. Ye, Z. W. Dai, C. Y. Qiu, M. Z. Ke, and Z. Y. Liu, Appl. Phys. Lett. **98**, 083505 (2011).
[11]A. E. Serebryannikov, K. B. Alici, T. Magath, A. O. Cakmak, and E. Ozbay, Phys. Rev. A **86**, 053835 (2012).
[12]A. V. Novitsky, V. M. Galynsky, and S. V. Zhukovsky, Phys. Rev. B **86**, 075138 (2012).
[13]V. Kuzmiak and A. A. Maradudin, Phys. Rev. A **86**, 043805 (2012).
[14]M. D. Tocci, M. J. Bloemer, M. Scalora, J. P. Dowling, and C. M. Bowden, Appl. Phys. Lett. **66**, 2324 (1995).
[15]V. V. Konotop and V. Kuzmiak, Phys. Rev. B **66**, 235208 (2002).
[16]B. Liang, B. Yuan, and J. C. Cheng, Phys. Rev. Lett. **103**, 104301 (2009).
[17]S. V. Zhukovsky and A. G. Smirnov, Phys. Rev. A **83**, 023818 (2011).
[18]S. Lepri and G. Casati, Phys. Rev. Lett. **106**, 164101 (2011).
[19]Z. F. Yu and S. H. Fan, Nat. Photonics **3**, 91–94 (2009).
[20]H. Lira, Z. F. Yu, S. H. Fan, and M. Lipson, Phys. Rev. Lett. **109**, 033901 (2012).
[21]L. J. Aplet and J. W. Carson, Appl. Opt. **3**, 544–545 (1964).
[22]R. J. Potton, Rep. Prog. Phys. **67**, 717–754 (2004).
[23]P. H. Siegel, IEEE Trans. Microwave Theory Tech. **50**, 910 (2002).
[24]B. Ferguson and X. C. Zhang, Nature Mater. **1**, 26–33 (2002).
[25]M. Tonouchi, Nat. Photonics **1**, 97–105 (2007).
[26]M. Liu, X. B. Yin, E. U. Avila, B. S. Geng, T. Zentgraf, L. Ju, F. Wang, and X. Zhang, Nature **474**, 64–67 (2011).
[27]A. N. Grigorenko, M. Polini, and K. S. Novoselov, Nat. Photonics **6**, 749–758 (2012).
[28]Q. L. Bao and K. P. Loh, ACS Nano **6**, 3677–3694 (2012).
[29]A. Ferreira, J. Viana-Gomes, Y. V. Bludov, V. Pereira, N. M. R. Peres, and A. H. Castro Neto, Phys. Rev. B **84**, 235410 (2011).
[30]I. Crassee, J. Levallois, A. L. Walter, M. Ostler, A. Bostwick, E. Rotenberg, T. Seyller, D. van der Marel, and A. B. Kuzmenko, Nat. Phys. **7**, 48–51 (2011).
[31]I. Crassee, M. Orlita, M. Potemski, A. L. Walter, M. Ostler, Th. Seyller, I. Gaponenko, J. Chen, and A. B. Kuzmenko, Nano. Lett. **12**, 2470–2474 (2012).
[32]A. Fallahi and J. Perruisseau-Carrier, Phys. Rev. B **86**, 195408 (2012).
[33]H. X. Da, Q. L. Bao, R. Sanaei, J. H. Teng, K. P. Loh, F. J. Garcia-Vidal, and C. W. Qiu, Phys. Rev. B **88**, 205405 (2013).
[34]J. A. Porto, F. J. García-Vidal, and J. B. Pendry, Phys. Rev. Lett. **83**, 2845 (1999).
[35]J. T. Shen and P. M. Platzman, Phys. Rev. B **70**, 035101 (2004).
[36]A. I. Fernández-Domínguez, F. J. García-Vidal, and L. Martín-Moreno, Phys. Rev. B **76**, 235430 (2007).
[37]X. R. Huang, R. W. Peng, and R. H. Fan, Phys. Rev. Lett. **105**, 243901 (2010).
[38]R. H. Fan, L. H. Zhu, R. W. Peng, X. R. Huang, D. X. Qi, X. P. Ren, Q. Hu, and M. Wang, Phys. Rev. B **87**, 195444 (2013).